Research Square

Preprints are preliminary reports that have not undergone peer review.
They should not be considered conclusive, used to inform clinical practice,
or referenced by the media as validated information.

Spatiotemporal Differentiation and Associated Factors of Urban Vitality in a Linear River-Valley City: A Case Study of Central Lanzhou

Huiyuan Guan

guanhy@lzjtu.edu.cn

Lanzhou Jiaotong University

Ze Yang

Lanzhou Jiaotong University

Xingzhen Zang

Gansu Provincial Transportation Planning and Design Institute Co., LTD.

De Wang

Tongji University

Minan Yang

Lanzhou Jiaotong University

Zhaoxuan Wang

Lanzhou Jiaotong University

Peichen Yang

Lanzhou Jiaotong University

Article

Keywords: urban vitality, river-valley linear city, subdistrict scale, LBS data, spatiotemporal differentiation

Posted Date: September 7th, 2026

DOI: https://doi.org/10.21203/rs.3.rs-10401711/v1

License: This work is licensed under a Creative Commons Attribution 4.0 International License.
Read Full License

Additional Declarations: No competing interests reported.

Spatiotemporal Differentiation and Associated Factors of Urban Vitality in a Linear River-Valley City: A Case Study of Central Lanzhou

Abstract: Urban vitality reflects the use of urban space and the concentration of human activities. However, the linear spatial structure shaped by river-valley topography may give urban vitality distinctive spatiotemporal characteristics, while its spatial differentiation and associated factors remain insufficiently identified. Taking subdistrict-level administrative units in the central urban area of Lanzhou as the analytical units, this study constructs an urban vitality index integrating activity volume and average dwell time based on location-based service activity data and multisource spatial data. Spatial statistical methods, GeoDetector, random forest modeling, and SHAP analysis are employed to examine spatial patterns and associated factors under different temporal contexts. The results show that urban vitality is characterized by high-value clustering in the central area of Chengguan District, localized high-value nodes along the east–west built-up area, and low values in peripheral subdistricts and towns. Overall vitality is higher on workdays than on rest days, with relatively high levels occurring during 06:00–12:00 and 12:00–18:00, respectively. Although vitality intensity varies over time, the direction of spatial extension, spatial centroid, and principal high-value areas remain generally stable, and significant positive spatial autocorrelation is observed across all temporal contexts. Public service, catering and accommodation, and transportation facilities are the major factors associated with urban vitality, although their explanatory power varies across temporal contexts. The joint explanatory power of most factor combinations exceeds that of either factor alone, while the random forest and SHAP results consistently indicate high predictive contributions from transportation and functional facilities. Distance to the Yellow River exhibits relatively low explanatory power and predictive contribution, indicating that river proximity has limited direct explanatory power for differences in urban vitality at the subdistrict scale. These findings provide a reference for optimizing transportation services, improving the spatial allocation of public services, and promoting differentiated spatial governance in river-valley linear cities.

Keywords: urban vitality; river-valley linear city; subdistrict scale; LBS data; spatiotemporal differentiation

1. Introduction

As urban development in China shifts from incremental expansion to urban renewal and the redevelopment of existing urban spaces (Deng et al., 2026; Li et al., 2023), the focus of urban vitality research has gradually shifted from static assessments of the spatial environment to the fine-grained identification of space-use processes, the state of human activities, and their spatiotemporal differentiation (Schläpfer et al., 2021; Cao et al., 2022). Urban vitality is an important indicator of the state of urban space use, reflecting the concentration and spatiotemporal mobility of human activities in urban space (Schläpfer et al., 2021). Human activities are unevenly distributed across different functional zones, transport corridors, and public service nodes within cities, while activity volume and dwell intensity often exhibit pronounced spatial differentiation (Sun and Jiang, 2024). Therefore, identifying the spatiotemporal differentiation of urban vitality within a specific urban spatial structure contributes to understanding the relationship between human activities and urban spatial organization and provides a basis for public service allocation, transport node optimization, and the renewal of existing urban spaces.

Early studies of urban vitality mainly focused on the relationship between the spatial environment and public activities, conceptualizing urban vitality as the capacity of the spatial environment to organize and support sustained human activities and emphasizing the roles of functional mix, appropriate spatial scale, pedestrian accessibility, and public space quality (Jacobs, 1992). Owing to limitations in data acquisition, related studies mostly relied on static data, including local surveys, demographic statistics, land-use data, and facility accessibility indicators. Although such data could reveal the relationship between the spatial environment and public activities, they were limited in their ability to continuously characterize actual activity intensity, dwell patterns, and their temporal variations at the urban scale (Cao et al., 2022). In recent years, multisource geospatial big data, including mobile phone location data (Ahas et al., 2015), social media check-in data (Wu et al., 2018), points of interest (POIs) and multidimensional built-environment data (Li et al., 2022), and street-view imagery (Wu et al., 2023), have gradually been applied to urban vitality research, promoting a shift in vitality measurement from single static indicators to an integrated representation of human activities, functional provision, the built environment, and spatial perception. On this basis, existing studies have further integrated multisource data to construct comprehensive frameworks for measuring urban vitality, thereby improving the spatial precision of vitality identification and its capacity for multidimensional representation (Wang et al., 2021; Tang et al., 2022), while activity data from multiple time periods have been used to reveal the temporal and spatial heterogeneity of urban vitality (Chen et al., 2023). Although related studies have expanded urban vitality measurement to include dimensions such as activity diversity, temporal diversity, and spatial diversity (Kang et al., 2021), the joint representation of activity volume and dwell characteristics, as well as the comprehensive identification of vitality differences across different temporal contexts, remains insufficiently explored.

The spatial differentiation of urban vitality is closely related to multidimensional built-environment factors, including functional facilities, transport conditions, development intensity, and spatial morphology (Yang and Wang, 2025). The relationship between built-environment factors and urban vitality is characterized by a certain degree of complexity: some factors may exhibit threshold effects within specific value ranges, and different factors may also interact with one another (Lee and Cho, 2025). Urban form results from the integrated configuration of spatial elements such as buildings, streets, and land parcels. Its overall structure not only affects the organization of urban functions and transport linkages but is also closely associated with the spatial distribution and clustering patterns of human activities (Chen et al., 2021). In cities strongly constrained by mountainous or river-valley terrain, the lateral expansion of built-up space is restricted, while transport corridors, public transport nodes, and functional facilities tend to be spatially concentrated along a limited set of axes and exhibit strong spatial coupling (Yang et al., 2024). Compared with cities located on plains and typical central urban areas, the spatiotemporal organization of urban vitality at the subdistrict scale and its associated factors in river-valley linear cities have not been sufficiently examined. Existing studies on Lanzhou have mainly examined road-network morphology and its association with urban vitality, while the joint roles and interactions of functional facilities, transport conditions, and built-space morphology have yet to be systematically identified (Lu et al., 2023). Lanzhou has a typical linear river-valley urban form, providing a representative empirical case for examining the characteristics of spatiotemporal differentiation in urban vitality and its associated factors under topographic constraints.

On this basis, taking the central urban area of Lanzhou as a case study, this study is conducted from two dimensions: spatiotemporal pattern identification and associated-factor analysis. It examines the spatial differentiation, directional extension, and local clustering of urban vitality across different

day types and intraday periods and compares the differences among various associated factors in terms of their spatial explanatory power and predictive contributions. Functional facilities, transport conditions, built-space morphology, and river-valley locational factors are incorporated into a unified analytical framework. GeoDetector is used to identify the explanatory power of each factor for the spatial differentiation of urban vitality and the interactions among these factors, while random forest and SHAP are employed to examine the predictive contributions of the variables and their nonlinear associations with urban vitality. This study focuses on the following questions: What patterns of spatial differentiation and clustering does subdistrict-level urban vitality in the central urban area of Lanzhou exhibit under different temporal contexts? What explanatory roles do functional facilities, transport conditions, built-space morphology, and river-valley locational factors play in differences in subdistrict-level urban vitality? Do multiple spatial factors exhibit interaction enhancement, and do their associations with subdistrict-level urban vitality show nonlinear characteristics? The findings can provide empirical evidence for understanding the spatial organization of urban vitality in river-valley linear cities and offer a reference for the optimization of existing urban spaces, public service allocation, and transport node optimization.

2. Study Area, Data Sources, and Methods

2.1 Study Area

Lanzhou is located in the upper reaches of the Yellow River in northwestern China and is the capital of Gansu Province and an important central city in the upper Yellow River region. The central urban area is constrained by the mountains to the north and south and the Yellow River valley, with construction land extending along a narrow east–west valley, exhibiting the typical characteristics of a linear river-valley city. This study determines the extent of the central urban study area according to the *Lanzhou Territorial Spatial Master Plan (2021–2035)* and uses subdistricts as the basic spatial units of analysis (Fig. 1). The study area covers the major built-up areas of Chengguan, Qilihe, Anning, and Xigu districts, as well as activity spaces along the Yellow River, and can support urban vitality measurement and associated-factor identification at the subdistrict scale.

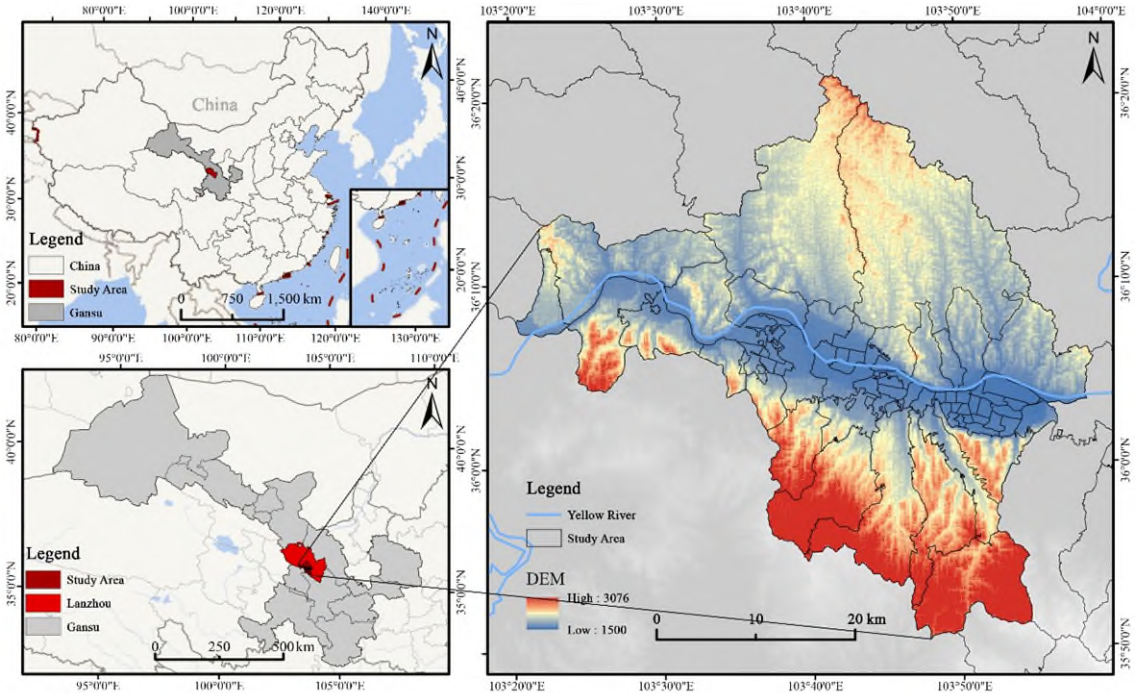


Fig. 1 Location and overview of the study area

2.2 Data Sources and Preprocessing

2.2.1 User Location Data from Location-Based Services (LBS)

The location-based services (LBS) data used in this study were provided by a mobile network operator and consist of mobile phone positioning data collected in Lanzhou over the one-month period from 1 to 31 May 2025. Based on the original trajectory sequence $S=\{(x_I, y_I, p_id_i)\}_{i=1}^{n}$, the speeds between consecutive points were calculated to suppress ping-pong drift caused by base-station switching; anomalous points with speeds exceeding 800 m/s were removed; and a dynamic circular buffer with a radius of 100 m was established to extract all non-empty p_id sequences within each segment, with the first entry used as the primary identifier. After processing, the trajectory data were converted into an alternating sequence of movement and stay events, and a stay event was identified when two adjacent spatiotemporal points both fell within the buffer. The processed dataset comprised more than 150 million user records and covered approximately 980,000 active mobile users in Lanzhou. The dataset contains user identifiers, latitude and longitude coordinates, timestamps, dwell duration, and other information. Tab. 1 presents the basic structure of the data sample. To ensure personal information security, all information involving user identity was de-identified. Because data from a single mobile operator may be influenced by user composition, device-use patterns, and positioning frequency, the LBS results are interpreted in this study as sample-based observations of activity intensity at the subdistrict scale rather than a complete enumeration of the activities of the entire population.

Tab. 1 Anonymous user sample data

uuid	longitude	latitude	start_time	stay_duration
00000366****b32e	103.8***	36.0***	2025/5/1 21:45:17	789
00000717****609b	103.8***	36.0***	2025/5/1 20:02:30	13308
.....	.....	.....	.....	.....
00007db****9d76	103.9***	36.0***	2025/5/30 12:07:39	28482
0000dca****f0dc	103.8***	36.0***	2025/5/30 0:28:29	10842
0000bd****a3f7	103.6***	36.4***	2025/5/31 13:25:45	10787

To reveal variations in urban vitality under different temporal contexts, the samples are organized according to two dimensions: day type and intraday period. Day types are divided into workdays and non-workdays, with non-workdays including weekends and statutory holidays, to distinguish routine commuting activities from non-workday activity states. Based on existing literature and residents' daily activity rhythms, the intraday period is divided into four intervals: 00:00–06:00, 06:00–12:00, 12:00–18:00, and 18:00–24:00, to compare variations in subdistrict-level urban vitality under different temporal contexts (Collins et al., 2024).

2.2.2 POI Data

The POI data were obtained from Amap (Gaode Maps), with a total of 86,203 POI records collected for the central urban area of Lanzhou in May 2025. The data attributes include name, category, latitude and longitude coordinates, and other information. The original POI data comprised 14 major categories, including business and residential services, hotel accommodation, and catering services, with each major category further divided into several secondary and tertiary categories (Tab. 2). To meet the needs of urban vitality research, records with unclear category information or weak associations with residents' daily activities were excluded, and the remaining data were organized and reclassified. Drawing on the findings of previous studies and the current Chinese *Standard for Urban Land Classification and Planning of Development Land* (GB 50137–2011), and considering the actual conditions of Lanzhou and the associated-factor indicator system used in this study, the POIs were classified into six first-level categories: commercial facilities, catering and accommodation facilities, leisure and entertainment facilities, public service facilities, office and employment facilities, and transport facilities.

Tab. 2 POI Reclassification details

First-Level Category	Second-Level Category	Examples
Commercial Facilities	Shopping and Consumption	Department stores, farmers' markets, vegetable markets, home-furnishing and building-material stores, etc.
	Daily-Life Services	Lottery outlets, laundries, printing shops, real-estate agencies, parcel collection points, etc.
Catering and Accommodation Facilities	Hotels and Accommodation	Youth hostels, hotels, homestays, hourly-rate rooms, etc.
	Food and Beverage Services	Fast-food restaurants, coffee shops, Western-style restaurants, cake shops, milk-tea shops, etc.
Transport Facilities	Automobile-Related Services	Auto-parts stores, auto-repair shops, used-car trading centers, car-rental services, etc.
	Transportation Facilities	Bus stops, parking lots, metro stations, railway stations, toll stations, etc.
Office and Employment Facilities	Companies and Enterprises	Offices, factory compounds, factories, office buildings, etc.
	Financial Institutions	Investment and wealth-management centers, insurance claims centers, banks, etc.
Public Service Facilities	Science, Education, and Culture	Archives, activity centers for retired cadres, universities, secondary schools, primary schools, kindergartens, etc.
	Medical and Healthcare Services	Centers for disease prevention and control, community hospitals, specialist hospitals, clinics, etc.
Leisure and Entertainment Facilities	Tourist Attractions	Zoos, forest parks, memorial halls, temples, parks, squares, etc.
	Leisure and Entertainment	Cinemas, agritainment venues, amusement parks, karaoke venues, etc.
	Sports and Fitness	Swimming pools, tennis courts, basketball courts, gyms, taekwondo clubs, etc.

2.3 Methods

2.3.1 Construction of the Urban Vitality Index

Urban vitality reflects the degree of concentration of human activities and the state of sustained use within subdistrict units. Using subdistrict-level administrative units as the basic spatial units, this study uses the number of LBS activity records per unit area to represent activity volume and the

average dwell duration to represent the degree of sustained use. To eliminate differences in measurement scales, the number of LBS activity records per unit area and the average dwell duration are subjected to min–max normalization, and a subdistrict-level urban vitality index is constructed using their product, as follows:

$$P_{it} = \frac{N_{it}}{A_i}$$

$$\mathrm{V_{it}} = \mathrm{P'_{it}} \times \mathrm{D'_{it}} \times 100$$

Where P_{it} denotes the number of LBS activity records per unit area in subdistrict i under temporal context t; N_{it} denotes the total number of LBS activity records in subdistrict i under temporal context t; A_i denotes the area of subdistrict i; V_{it} denotes the urban vitality level of subdistrict i under temporal context t; and $\mathrm{P'_{it}}$ and $\mathrm{D'_{it}}$ denote the min–max-normalized activity volume and dwell intensity, respectively. The index is used to jointly characterize the volume of human activities and sustained dwell characteristics within subdistrict units.

2.3.2 Spatial Pattern Analysis of Urban Vitality

(1) Standard Deviational Ellipse Analysis

The standard deviational ellipse is used to characterize the mean center, dispersion range, and directional trend of the spatial distribution of geographic features (Yuill, 1971). In this study, the subdistrict-level urban vitality index is used as the weight to calculate, under different temporal contexts, the weighted mean center, major axis, minor axis, and directional angle of the urban vitality distribution, in order to identify the dominant direction of its spatial distribution and its temporal differences. The weighted mean center is calculated as follows:

$$\bar{x} = \frac{\sum w_i x_i}{\sum w_i}, \quad \bar{y} = \frac{\sum w_i y_i}{\sum w_i}$$

Where (x_i, y_i) denotes the spatial location of subdistrict i, w_i denotes its urban vitality value, and $(\bar{x}, \bar{y})$ denotes the weighted mean center of the urban vitality distribution. The major axis of the ellipse reflects the primary direction of urban vitality extension, the minor axis reflects the secondary direction of extension, and the area of the ellipse represents the degree of spatial dispersion of the urban vitality distribution. Given the linear river-valley spatial characteristics of Lanzhou, this method can be used to determine whether subdistrict-level urban vitality exhibits a spatial trend of extension along the direction of the river valley.

(2) Spatial Autocorrelation Analysis

Spatial autocorrelation analysis is used to test the spatial dependence of subdistrict-level urban vitality. In this study, global Moran's I is used to assess the overall degree of clustering of subdistrict-level urban vitality in the central urban area of Lanzhou, and local Moran's I is used to identify local clustering and types of spatial outliers (Anselin et al., 2006).

Global Moran's I is calculated as follows:

$$I = \frac{n}{S_0} \frac{\sum_{i=1}^{n} \sum_{j=1}^{n} w_{ij}(x_i - \bar{x})(x_j - \bar{x})}{\sum_{i=1}^{n} (x_i - \bar{x})^2}$$

Where n is the number of subdistricts; x_i and x_j are the urban vitality values of subdistricts i and j, respectively; $\bar{x}$ is the mean urban vitality value; w_{ij} is the spatial weight; and S_0 is the sum of the spatial weights. $I > 0$ indicates that similar urban vitality levels tend to cluster spatially,

$I < 0$ indicates that adjacent subdistricts tend to have substantially different urban vitality levels, and I close to 0 indicates that the spatial distribution tends to be random.

Local Moran's I is calculated as follows:

$$I_i = z_i \sum_{j=1}^{n} w_{ij} z_j$$

Where I_i is the local indicator of spatial association for subdistrict i, and z_i and z_j are the standardized urban vitality values of subdistricts i and j, respectively. Based on significance testing, local spatial associations are classified into four types: high–high clustering, low–low clustering, high–low outliers, and low–high outliers.

2.3.3 Analysis of Factors Associated with Urban Vitality

(1) GeoDetector Analysis

This study uses the factor detector and interaction detector of GeoDetector to analyze the explanatory power of each factor for the spatial differentiation of subdistrict-level urban vitality and the interactions among these factors. This method does not rely on linear assumptions and is suitable for identifying factors associated with spatial differentiation (Wang et al., 2016). The factor detector uses the q value to measure the explanatory power of an individual factor, and the q value is calculated as follows:

$$q = 1 - \frac{\sum_{h=1}^{L} N_h \sigma_h^2}{N\sigma^2}$$

Where N and σ^2 denote the total number of subdistricts and the overall variance of urban vitality, respectively; N_h and σ_h^2 denote the number of subdistricts in stratum h and the variance of urban vitality in stratum h, respectively; and L denotes the number of strata. The q value takes values within [0,1], with a larger value indicating stronger explanatory power of the factor for the spatial differentiation of subdistrict-level urban vitality.

The interaction detector is used to assess whether the joint effect of factors X_1 and X_2 enhances or weakens the explanatory power for the dependent variable Y, or whether the effects of the two factors on Y are independent of each other. For this assessment, $q(X_1)$, $q(X_2)$, and $q(X_1 \cap X_2)$ are calculated separately, and their magnitudes are compared.

(2) Random Forest Regression and SHAP-Based Interpretation

To further verify the dominant factors identified by GeoDetector and analyze the contribution of each variable to the prediction of subdistrict-level urban vitality, this study constructs a random forest regression model. Random forest generates multiple regression trees by randomly sampling observations and candidate features, and uses the average of the predictions of all trees as the final predicted value (Kalange et al., 2022).

$$\hat{Y}i = \frac{1}{B}\sum b = 1^{B} T_b(X_i)$$

Where $\hat{Y}_i$ denotes the predicted urban vitality value of subdistrict i, B denotes the number of regression trees, and $T_b(X_i)$ denotes the prediction of the bth regression tree for subdistrict i. Models are constructed separately with subdistrict-level urban vitality on workdays, non-workdays, and during the two representative periods as the dependent variable in each model, and five-fold cross-validation is used to evaluate the predictive performance of the models.

On this basis, the SHAP method is used to explain the contribution of each associated factor to model predictions. Based on the concept of additive feature attribution, SHAP decomposes the prediction for an individual sample into the sum of a baseline value and the contribution values of all variables (Lundberg et al., 2020).

$$f(x) = \phi_0 + \sum_{j=1}^{M} \phi_j$$

Where $f(x)$ denotes the model prediction, ϕ_0 denotes the baseline prediction, and ϕ_j denotes the SHAP value of the jth variable. A positive SHAP value indicates that the variable increases the predicted value relative to the baseline value, whereas a negative SHAP value indicates that the variable decreases the predicted value. The mean absolute SHAP value of a variable reflects its overall predictive contribution, while the distribution of SHAP values is used to identify the contribution direction and nonlinear variation characteristics represented by the model. The relevant results represent only variable contributions in a predictive sense and are not used as a basis for determining causal relationships.

2.3.4 Robustness Tests

To examine the sensitivity of the research conclusions to model specification, robustness tests are conducted from two aspects: the spatial weights matrix and the variable discretization method. In the spatial autocorrelation analysis, the Queen contiguity matrix is used as the baseline, and global Moran's I is recalculated using the Rook contiguity matrix. Queen contiguity defines subdistricts sharing a common edge or vertex as neighboring units, whereas Rook contiguity considers only subdistricts sharing a common edge. If the sign, significance, and temporal variation patterns of Moran's I are generally consistent across different spatial weights matrices, the conclusion regarding the spatial clustering of subdistrict-level urban vitality is considered insensitive to the contiguity rule (Stakhovych and Bijmolt, 2009).

GeoDetector requires continuous explanatory variables to be discretized before entering the model, and the discretization method may affect the (q) values and factor rankings. Classification into four categories using the quantile method is used as the baseline, and classification into four categories using the natural breaks method is used for comparison. If the significant factors, dominant factors, and their overall rankings are generally consistent under the two discretization methods, the results of factor identification are considered robust to different variable discretization methods (Song et al., 2020).

3. Multiscale Evolutionary Characteristics of Urban Vitality Spatiotemporal Patterns

3.1 Overall Spatial Differentiation Pattern of Subdistrict-Level Urban Vitality

Subdistrict-level urban vitality in the central urban area of Lanzhou exhibits an uneven spatial distribution, with subdistricts showing high vitality values mainly concentrated in the core area of Chengguan District, localized high values occurring in the western built-up area, and generally low vitality levels in peripheral subdistricts (Fig. 2). On workdays, the subdistrict-level urban vitality index ranges from 0.00 to 74.96, with a mean of 25.03. High-vitality subdistricts mainly include Jiuquan Road, Linxia Road, Zhangye Road, and Railway East Village, which are concentrated in the core area of Chengguan District; Xigucheng appears as a relatively independent high-vitality subdistrict in the western part of the study area. On rest days, the subdistrict-level urban vitality index ranges from 0.00

to 62.70, with a mean of 22.70. High-vitality subdistricts remain mainly concentrated in the core area of Chengguan District, with Linxia Road, Jiuquan Road, and Zhangye Road maintaining relatively high levels, while Xigucheng continues to exhibit a localized high value in the western part of the study area. Both the maximum and mean values of the vitality index are lower on rest days than on workdays, but the spatial locations of the main high- and low-vitality subdistricts are generally similar between the two types of days. The differences between workdays and rest days are mainly reflected in the levels of the vitality index, while the basic spatial structure of subdistrict-level urban vitality remains generally similar.

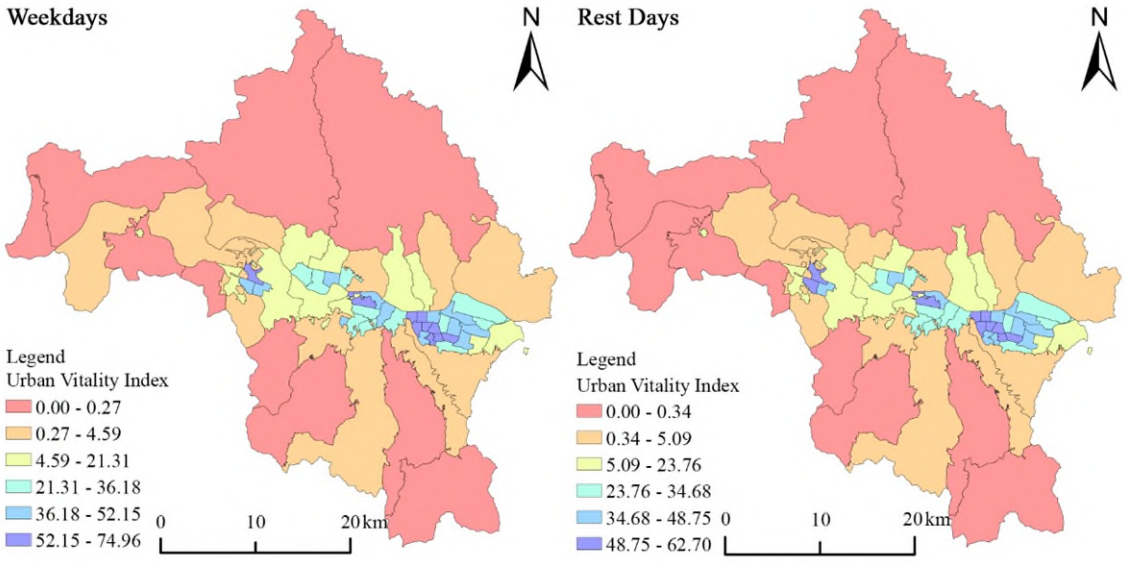


Fig. 2 Overall Spatial Distribution of Urban Vitality

3.2 Intraday Differences in Urban Vitality between Workdays and Rest Days

Subdistrict-level urban vitality levels vary across different periods, but the main spatial locations of high- and low-vitality subdistricts are generally similar (Fig. 3). Across all periods, low-vitality subdistricts are mainly distributed along the periphery of the study area, while high-vitality subdistricts are concentrated in the core area of Chengguan District, with Xigucheng and other western subdistricts forming localized high values. On workdays, the mean vitality level during 06:00–12:00 is the highest among the four periods, with the maximum value of the urban vitality index reaching 92.97, while subdistricts in the core area of Chengguan District, including Zhangye Road, Jiuquan Road, and Linxia Road, fall within relatively high vitality categories. On rest days, 12:00–18:00 is a period of relatively high vitality, with high-vitality subdistricts still mainly concentrated in the core area of Chengguan District and showing a more concentrated spatial distribution than during the same period on workdays. Differences across temporal contexts are mainly reflected in changes in subdistrict-level vitality levels and the distribution of localized high values, while the basic spatial pattern of high values in the Chengguan core area and low values in peripheral areas remains generally similar.

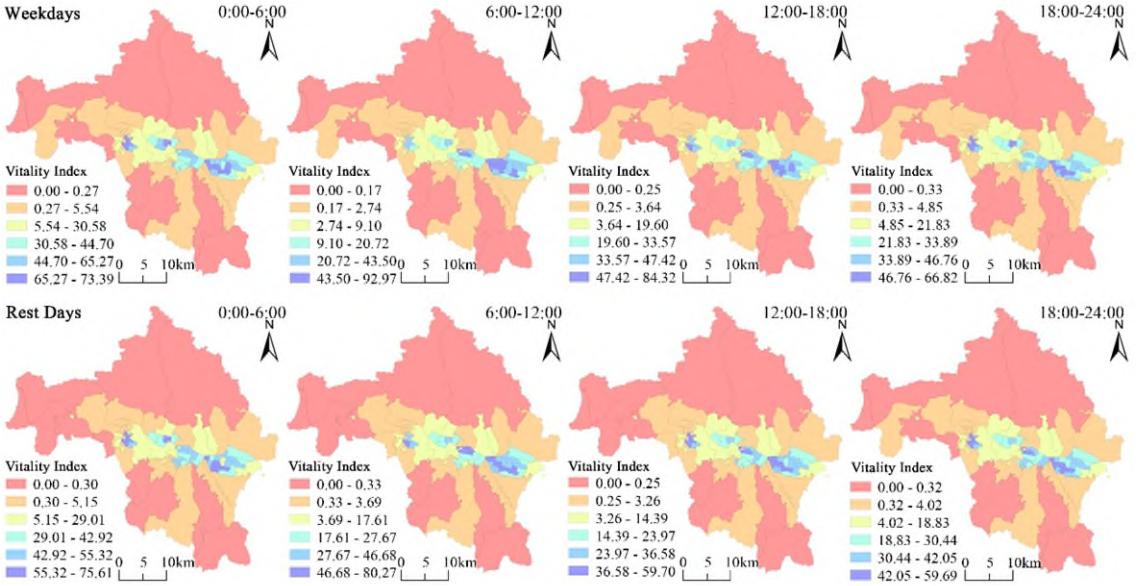


Fig. 3 Urban Vitality across Different Time Periods

3.3 Spatial Directionality and Mean-Center Shifts of Urban Vitality

Across all temporal contexts, the directional angles of the standard deviational ellipses for subdistrict-level urban vitality range from 106.70° to 107.02°, with a range of only 0.32°. The major axes extend approximately east–west, which is generally consistent with the extension direction of Lanzhou's linear built-up space (Fig. 4). On workdays, the major- and minor-axis standard distances range from 10.70 to 12.11 km and from 1.93 to 2.24 km, respectively, while on rest days they range from 11.44 to 12.13 km and from 2.02 to 2.20 km, respectively. The spatial dispersion scales of the vitality distribution are generally similar between the two types of days, although the intraday variations in the major and minor axes are relatively greater on workdays. The mean centers for all periods are located near the core area of Chengguan District, and the maximum displacement between adjacent periods is 1.37 km, occurring between 00:00–06:00 and 06:00–12:00 on workdays. The dominant direction of subdistrict-level urban vitality extension remains generally stable, and differences across temporal contexts are mainly reflected in the spatial dispersion scale and localized shifts of the mean center.

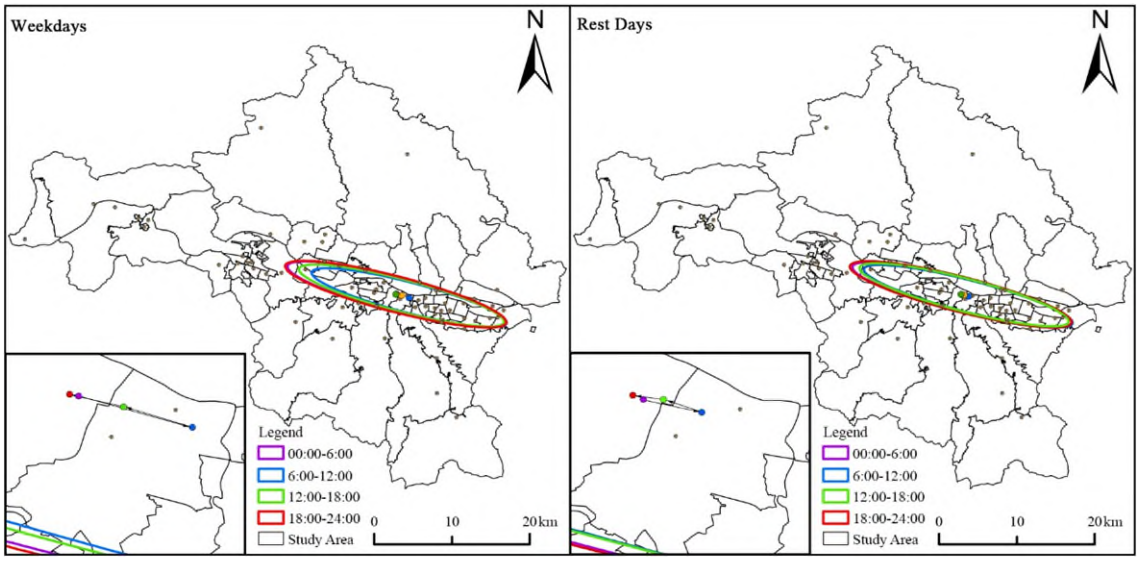


Fig. 4 Mean-Center Shift Trajectories of Urban Vitality

3.4 Global Spatial Autocorrelation Characteristics of Urban Vitality

To examine the global spatial autocorrelation of subdistrict-level urban vitality, the Queen contiguity matrix is used to calculate global Moran's I under different temporal contexts, and the Rook contiguity matrix is used to test the robustness of the results. Under the Queen contiguity matrix, Moran's I values range from 0.4811 to 0.5409 across all temporal contexts and are all significant at the 0.1% level, indicating significant positive spatial autocorrelation in subdistrict-level urban vitality in the central urban area of Lanzhou (Tab. 3). The Moran's I values for 06:00–12:00 on workdays and 12:00–18:00 on rest days are 0.5409 and 0.4978, respectively, both of which are the highest among the four periods within the corresponding day type, indicating that the degree of global spatial clustering of subdistrict-level urban vitality is relatively higher during the morning on workdays and the afternoon on rest days, respectively. Under the Rook contiguity matrix, Moran's I values remain positive and significant at the 0.1% level across all temporal contexts, and the absolute differences from the corresponding Moran's I values obtained using the Queen contiguity matrix do not exceed 0.0016. The signs, significance levels, and overall temporal variation patterns are generally consistent between the two matrices, indicating that the global spatial autocorrelation results are insensitive to the contiguity rule and demonstrate good robustness.

Tab. 3 Global Moran's I of Urban Vitality under Different Temporal Contexts and Robustness Test Results

Day Type	Time Period	Queen Moran's I	z-value	p-value	Rook Moran's I	Rook p-value	Robustness Test
workdays	00:00—06:00	0.4848	6.6186	<0.001	0.4835	<0.001	Consistent
workdays	06:00—12:00	0.5409	7.5568	<0.001	0.5406	<0.001	Consistent
workdays	12:00—18:00	0.5020	6.9227	<0.001	0.5013	<0.001	Consistent
workdays	18:00—24:00	0.4811	6.5769	<0.001	0.4795	<0.001	Consistent
Rest days	00:00—06:00	0.4873	6.6597	<0.001	0.4859	<0.001	Consistent
Rest days	06:00—12:00	0.4872	6.7258	<0.001	0.4864	<0.001	Consistent
Rest days	12:00—18:00	0.4978	6.8392	<0.001	0.4967	<0.001	Consistent
Rest days	18:00—24:00	0.4822	6.5947	<0.001	0.4808	<0.001	Consistent

3.5 Local Spatial Clustering and Spatial Outlier Identification of Urban Vitality

Building on the global Moran's I test, local Moran's I is further calculated using the Queen contiguity matrix, and LISA cluster maps are produced to identify local spatial clustering and spatial outlier types of subdistrict-level urban vitality. Across different temporal contexts, the numbers of subdistricts classified as high–high and low–low clusters range from 8 to 10 and from 13 to 15,

respectively, and together these two types of same-value clusters account for 95.5%–100% of the units with significant local spatial associations. Only one low–high outlier is identified in each of four temporal contexts, and no significant high–low outliers are identified, indicating that the significant types of local spatial association are dominated by same-value clustering (Fig. 5). High–high clusters are mainly distributed in the core area of Chengguan District. Among them, five subdistricts exhibit the high–high type across all eight temporal contexts, forming a relatively stable core of high-vitality clustering during the study period. Low–low clusters are mainly located along the periphery of the study area. A total of 13 subdistricts exhibit the low–low type across all eight temporal contexts, and these subdistricts form several contiguous clustering areas along the northern, western, and southern margins. Both 06:00–12:00 on workdays and 12:00–18:00 on rest days exhibit a local spatial structure characterized by the coexistence of high–high clusters in the Chengguan core area and low–low clusters in peripheral areas, further locating the main local clustering areas corresponding to the global positive spatial autocorrelation.

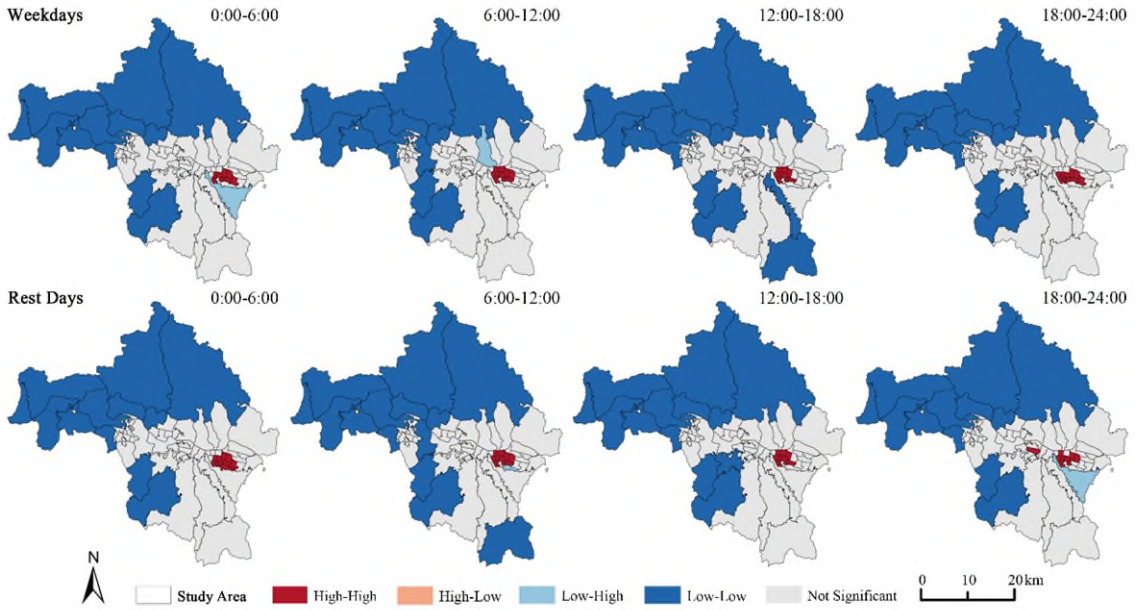


Fig. 5 LISA Cluster Maps of Urban Vitality under Different Temporal Contexts

4. Detection of Factors Associated with Urban Vitality and Spatial Diagnosis

4.1 Selection of Influencing Factors and Data Processing

Based on existing studies of urban vitality and the built environment (Li et al., 2022), and considering the spatial characteristics of Lanzhou's linear development within the river valley, four categories of associated factors—functional environment, transport environment, spatial morphology, and river-valley location—are selected to construct the indicator system (Tab. 4). The functional environment is represented by the densities of commercial, dining and accommodation, leisure and entertainment, public service, and office and employment facilities, and is used to reflect the provision of functional facilities and potential activity opportunities within each subdistrict. The transport environment includes transport facility density, bus stop density, and road network density, which respectively reflect the configuration of transport service facilities, public transport stops, and the road network. Spatial morphology is represented by the building coverage ratio, which reflects the extent of building footprint coverage within each subdistrict, while river-valley location is measured by the shortest distance from the subdistrict centroid to the Yellow River channel. POI and bus stop densities

are calculated as the ratios of the numbers of corresponding facilities to the subdistrict area; road network density is calculated as the ratio of total road length to the subdistrict area; and the building coverage ratio is calculated as the ratio of building footprint area to the subdistrict area. GeoDetector requires explanatory variables to be entered in categorical form. Considering that the study area contains 65 subdistrict-level units, each continuous factor is divided into four categories using the quantile method to avoid excessively small sample sizes within categories and maintain comparability across different temporal contexts. The classification criteria for each factor are kept consistent across temporal contexts. The natural breaks method with four categories is also used to test the sensitivity of the results to the discretization method.

Tab. 4 Indicator System and Classification of Factors Associated with Urban Vitality

Factor Category	Associated Factor	Calculation Method	Code
Functional Environment	Commercial facility density (No./km²)	Number of commercial POIs / subdistrict area	X1
	Dining and accommodation facility density (No./km²)	Number of dining and accommodation POIs / subdistrict area	X2
	Leisure and entertainment facility density (No./km²)	Number of leisure and entertainment POIs / subdistrict area	X3
	Public service facility density (No./km²)	Number of public service POIs / subdistrict area	X4
	Office and employment facility density (No./km²)	Number of office and employment POIs / subdistrict area	X5
Transport Environment	Transport facility density (No./km²)	Number of transport facility POIs / subdistrict area	X6
	Bus stop density (No./km²)	Number of bus stops / subdistrict area	X7
	Road network density (km/km²)	Total road length / subdistrict area	X8
Spatial Morphology	Building coverage ratio (km²/km²)	Building footprint area / subdistrict area	X9
River-Valley Location	Distance to the Yellow River (m)	Shortest distance from the subdistrict centroid to the Yellow River channel	X10

4.2 Identification of the Explanatory Power of Associated Factors under Different Temporal Contexts

The factor detector module of GeoDetector is used to measure the explanatory power of individual associated factors for the spatial differentiation of subdistrict-level urban vitality. Except for the distance to the Yellow River, X1–X9 are significant at the 1% level across all temporal contexts, and most functional-facility and transport-facility indicators have relatively high (q) values. The (q) value for the distance to the Yellow River ranges only from 0.054 to 0.073, indicating limited single-factor explanatory power (Tab. 5). For the overall workday and rest-day contexts, the composition of the three highest-ranking factors in terms of (q) values is the same, comprising public service facility density, dining and accommodation facility density, and transport facility density. The factor rankings based on (q) values differ between the two representative periods. During 06:00–12:00 on workdays, office and employment facility density, commercial facility density, and transport facility density rank among the top three, with (q) values of 0.805, 0.802, and 0.765, respectively. During 12:00–18:00 on rest days, public service facility density, dining and accommodation facility density, and transport facility density rank among the top three, with (q) values of 0.846, 0.813, and 0.802, respectively. Overall, the main explanatory factors are relatively consistent between the overall workday and rest-day contexts, whereas the factor rankings and composition show some differences between the representative periods.

Tab. 5 Explanatory Power of Individual Urban Vitality Factors across Temporal Contexts

Factor	Workdays	Rest Days	Workdays 06:00—12:00	Rest Days 12:00—18:00
X1	0.829	0.820	**0.802**	0.784
X2	**0.851**	**0.847**	0.754	**0.813**
X3	0.822	0.820	0.657	0.792
X4	**0.871**	**0.859**	0.736	**0.846**
X5	0.840	0.824	**0.805**	0.797
X6	**0.852**	**0.839**	**0.765**	**0.802**
X7	0.835	0.827	0.683	0.789
X8	0.677	0.679	0.438	0.646

X9	0.815	0.815	0.643	0.738
X10	0.073	0.066	0.054	0.061

Note:Values in the table are (q) values. Bold values indicate the three factors with the highest explanatory power under each temporal context. Definitions of X1–X10 are provided in Tab. 4.

To examine the sensitivity of the factor detection results to the discretization method, the natural breaks method is further adopted for comparison. Under the different discretization methods, the three highest-ranking factors in terms of (q) values are generally similar within each temporal context and mainly include indicators related to public services, dining and accommodation, commercial facilities, office and employment, transport facilities, and spatial morphology (Tab. 6). The three highest-ranking factors are identical between the two discretization methods in both the overall workday context and the 12:00–18:00 rest-day context, while two of the three factors overlap between the two methods in both the overall rest-day context and the 06:00–12:00 workday context. Although the rankings and composition of some factors change, factors with high explanatory power continue to fall mainly within the categories of functional environment, transport environment, and spatial morphology, indicating that the main factor detection results exhibit a certain degree of robustness to the discretization method.

Tab. 6 Robustness Test of the Explanatory Power of Dominant Factors under Different Discretization Methods

Temporal Context	Quantile Method	Natural Breaks Method	Robustness Test
Workdays	X4 (0.871) X6 (0.852) X2 (0.851)	X6 (0.915) X4 (0.850) X2 (0.848)	The dominant factors are highly consistent
Rest Days	X4 (0.859) X2 (0.847) X6 (0.839)	X6 (0.895) X2 (0.836) X9 (0.826)	Factors with high explanatory power remain concentrated in transport, consumption-related facilities, and the built environment
Workdays 06:00–12:00	X5 (0.805) X1 (0.802) X6 (0.765)	X4 (0.870) X1 (0.861) X5 (0.859)	Commercial, office and employment, and service-related factors retain high explanatory power
Rest Days 12:00–18:00	X4 (0.846) X2 (0.813) X6 (0.802)	X6 (0.886) X2 (0.870) X4 (0.870)	The dominant factors are highly consistent

Note: Only the three factors with the highest (q) values under each temporal context are listed. The quantile method is used as the baseline discretization method, while the natural breaks method is used for the robustness test.

4.3 Enhancement Effects of Multi-Factor Interactions on Urban Vitality

Building on the single-factor detection results, the interaction detector is further used to identify the joint explanatory power of different combinations of associated factors for the spatial differentiation of subdistrict-level urban vitality. Under the two representative temporal contexts of 06:00–12:00 on workdays and 12:00–18:00 on rest days, the interaction (q) values of most combinations are higher than those of the individual factors comprising each combination, indicating that pairwise factor combinations have greater joint explanatory power (Fig. 6). During 06:00–12:00 on workdays, the interaction (q) values of X5∩X1, X5∩X2, and X5∩X3 all exceed 0.85. The combinations of office and employment facility density with commercial, dining and accommodation, and leisure and entertainment facility densities exhibit relatively high explanatory power. During 12:00–18:00 on rest days, the interaction (q) values of X8∩X4, X8∩X2, and X8∩X6 are approximately 0.91, 0.89, and 0.88, respectively. The combinations of road network density with public service facility density, dining and accommodation facility density, and transport facility density exhibit relatively high explanatory power. Overall, factor combinations with high (q) values during workday mornings mainly involve office and employment facilities and multiple types of functional facilities, whereas those during the afternoon on rest days mainly consist of combinations

of the road network with service, consumption-related, and transport facilities. This indicates that the composition of factor combinations with high explanatory power differs across temporal contexts.

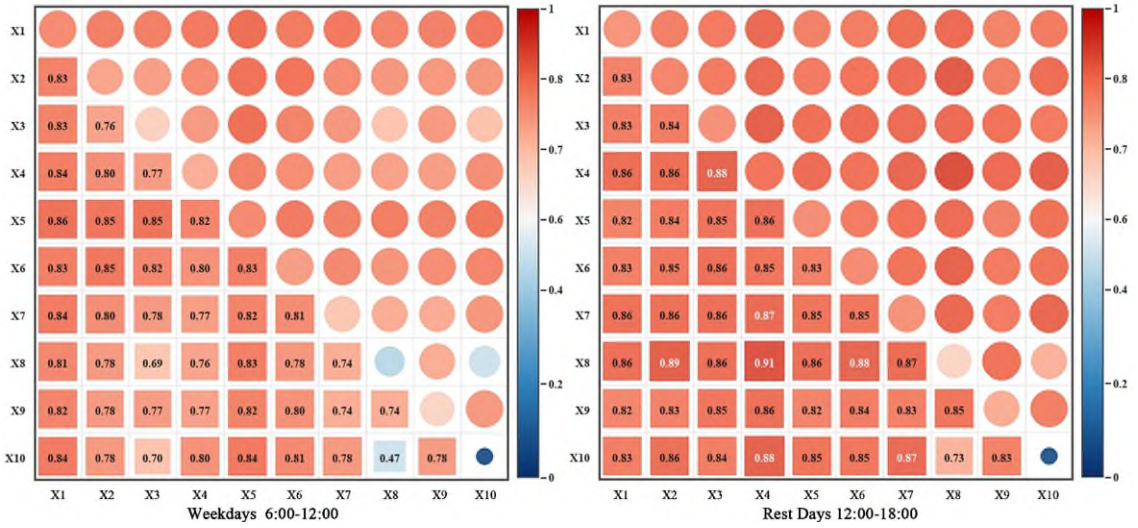


Fig. 6 Interaction Detection of Urban Vitality Factors under Representative Temporal Contexts

4.4 Random Forest Variable Importance and SHAP Interpretation

To further examine the predictive relationships between the associated factors and subdistrict-level urban vitality within a continuous-variable framework, random forest regression models are constructed, and variable importance and SHAP values are used to analyze the predictive contribution of each variable under different temporal contexts. The five-fold cross-validation results show that the mean R^2 values of the models for the four temporal contexts range from 0.906 to 0.930. The overall workday model yields the highest mean R^2, whereas the 06:00–12:00 workday model yields a relatively lower value (Tab. 7). The MAE values of the models range from 2.894 to 3.530, while the RMSE values range from 4.473 to 6.393, indicating that the random forest models provide a good fit to the variation in subdistrict-level urban vitality within the current sample, thereby providing a model basis for the subsequent variable-importance and SHAP analyses.

Tab. 7 Predictive Performance of the Random Forest Models

Response Variable	Test-Set R^2	MAE	RMSE	R^2
Workdays	0.930	3.530	5.560	0.988
Rest Days	0.918	3.420	5.231	0.983
Workdays 06:00–12:00	0.906	3.468	6.393	0.984
Rest Days 12:00–18:00	0.917	2.894	4.473	0.985

Note: The test-set evaluation metrics reported in the table are the mean values obtained from five-fold cross-validation. MAE denotes mean absolute error, and RMSE denotes root mean square error.

The random forest variable-importance results show that the composition of the top-ranking variables is relatively consistent between the overall workday and rest-day models. Bus stop density (X7) ranks first in both models, while transport facility density (X6), dining and accommodation facility density (X2), and public service facility density (X4) also exhibit relatively high importance (Fig. 7). The variable-importance structures differ between the representative periods. In the 06:00–12:00 workday model, variable importance is mainly concentrated in office and employment facility density (X5) and commercial facility density (X1), with the importance of office and employment facility density reaching 42.8%. In the 12:00–18:00 model for rest days, the importance values of dining and accommodation facility density, public service facility density, and transport facility density are relatively similar. By comparison, road network density (X8), building coverage ratio (X9),

and distance to the Yellow River (X10) generally show relatively low importance across the four models, with the importance of distance to the Yellow River remaining below 1% in all models. Overall, variables related to transport and functional service facilities show relatively high predictive contributions in the overall workday and rest-day models, whereas the composition of high-importance variables in the representative-period models varies across temporal contexts.

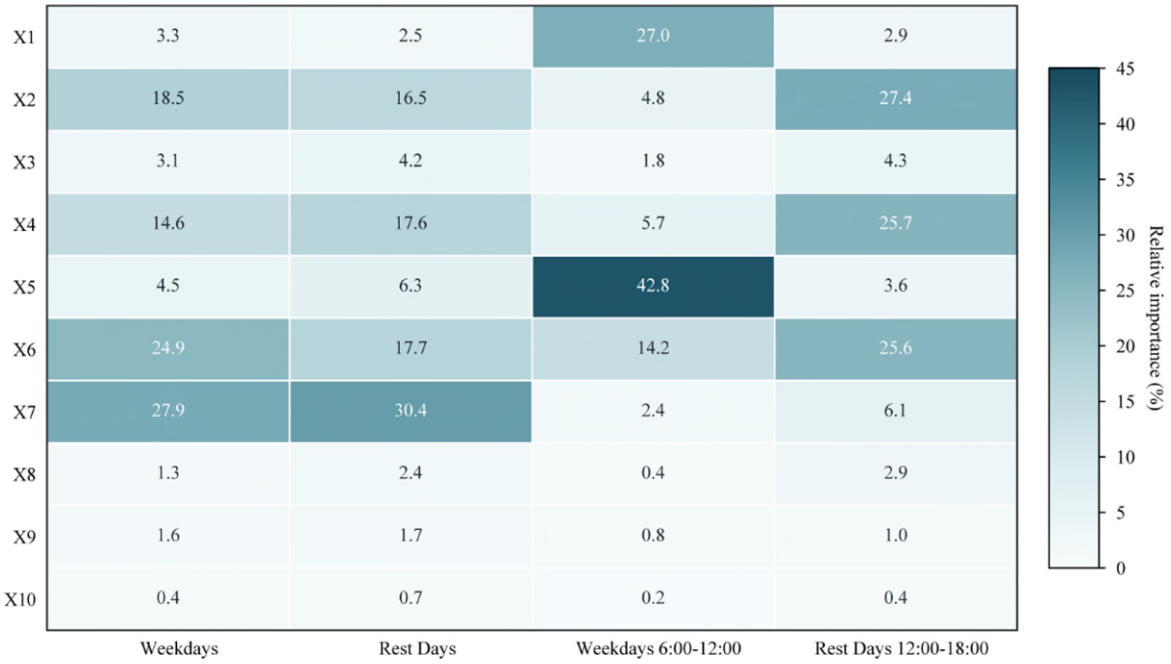


Fig. 7 Heatmap of Random Forest Relative Variable Importance across Temporal Contexts

The SHAP analysis further reveals the directions and distributional characteristics of the contributions of the values of each variable to the predicted values of subdistrict-level urban vitality (Fig. 8). Positive SHAP values indicate that the corresponding variable values increase the model's predicted values, whereas negative SHAP values indicate that they decrease the predicted values. In the overall models for workdays and rest days, bus stop density (X7), transport facility density (X6), public service facility density (X4), and dining and accommodation facility density (X2) all exhibit relatively large ranges of SHAP values. Observations with high values of these variables are mostly distributed within the positive SHAP-value range, indicating that higher values of these variables generally correspond to higher predicted values of subdistrict-level urban vitality. During the representative periods, the directions of variable contributions show different characteristics. In the model for 06:00–12:00 on workdays, observations with high values of office and employment facility density (X5) and commercial facility density (X1) mainly correspond to positive SHAP values. In the model for 12:00–18:00 on rest days, observations with high values of dining and accommodation facility density (X2), public service facility density (X4), and transport facility density (X6) are mostly distributed within the positive SHAP-value range. Overall, the SHAP results correspond to the variable-importance analysis and further indicate that both the composition of variables with high predictive contributions and the relationships between their values and the predicted values of subdistrict-level urban vitality differ across temporal contexts.

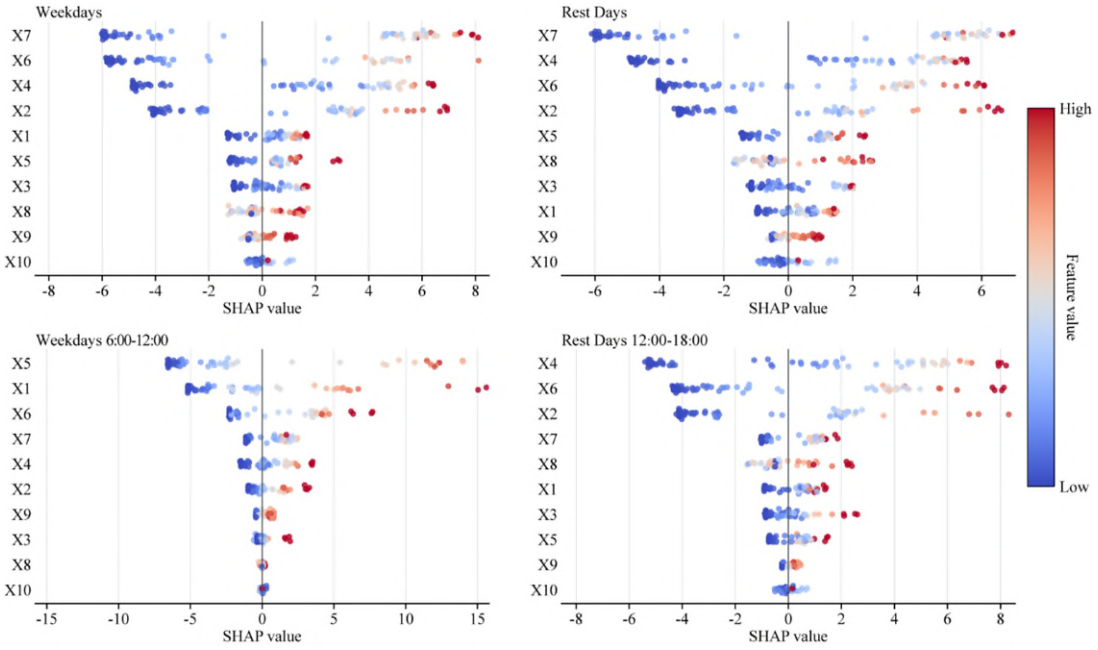


Fig. 8 SHAP Results for Urban Vitality Factors across Temporal Contexts

Taken together, the random forest variable-importance and SHAP results show that bus stop density (X7), transport facility density (X6), public service facility density (X4), and dining and accommodation facility density (X2) make relatively high contributions to model predictions in most temporal contexts and constitute a relatively consistent set of high-contribution variables across different contexts. Office and employment facility density (X5) and commercial facility density (X1), however, rank relatively high in the model for 06:00–12:00 on workdays, indicating that the composition of high-contribution variables differs to some extent across temporal contexts. Both the random forest and GeoDetector results highlight the importance of variables related to the transport environment and functional facilities, although the specific rankings of the variables differ. The two methods provide complementary results from the perspectives of prediction based on continuous variables and the explanation of spatial differentiation. Random forest variable importance and SHAP values reflect the relative contributions of variables to model predictions and are not used as a basis for determining causal relationships.

5. Conclusions and Discussion

5.1 Conclusions

This study focuses on the central urban area of Lanzhou and uses LBS activity data and multisource geospatial data to measure urban vitality at the subdistrict scale from the two dimensions of activity volume and stay intensity. The study analyzes the spatial differentiation, directional extension, and local clustering characteristics of urban vitality across different day types and intraday periods. It also examines the factors associated with urban vitality from the two perspectives of the explanation of spatial differentiation and model prediction. The main conclusions are as follows:

(1) Urban vitality at the subdistrict scale in the central urban area of Lanzhou exhibits a markedly uneven spatial distribution. High-vitality subdistricts are mainly concentrated in the central Chengguan area, while several local high-value nodes are distributed within the east–west built-up area. In contrast, the peripheral subdistricts and towns generally exhibit lower vitality, reflecting

relatively pronounced spatial differentiation between the central area and the peripheral subdistricts and towns.

(2) Across different temporal contexts, subdistrict-level urban vitality is characterized by the coexistence of variations in intensity and stability in spatial structure. Overall urban vitality is higher on workdays than on rest days, with 06:00–12:00 on workdays and 12:00–18:00 on rest days representing periods of relatively high vitality for the two day types, respectively. Across all temporal contexts, the distribution of urban vitality extends in an east–west direction, while the directional angle and mean center vary only slightly, and significant positive spatial autocorrelation is observed. High–high cluster areas are mainly distributed in the central Chengguan area, whereas low–low cluster areas are concentrated in the peripheral subdistricts and towns.

(3) The main factors associated with subdistrict-level urban vitality are generally stable, although their explanatory power and predictive contributions vary across day types and intraday periods. Public service, dining and accommodation, and transport facilities all have relatively high explanatory power in the overall workday and rest-day contexts. During workday mornings, office and employment facilities and commercial facilities are more important, whereas public service, dining and accommodation, and transport facilities are the main associated factors during afternoons on rest days. The joint explanatory power of interacting factors is generally higher than the explanatory power of individual factors, indicating that the spatial differentiation of subdistrict-level urban vitality exhibits a pronounced interaction-enhancement pattern. The types of high-contribution variables identified by the random forest and SHAP analyses are generally consistent with the GeoDetector results, further highlighting the importance of transport conditions and functional facilities. Both the spatial explanatory power and predictive contribution of the distance to the Yellow River are relatively low, and under the current analytical framework, river proximity did not emerge as a direct dominant factor explaining differences in subdistrict-level urban vitality.

5.2 Discussion

Influenced by its river-valley topography, Lanzhou has developed an east–west linear urban space. Natural geographical conditions are closely related to the layout of urban construction land and transport systems in mountainous cities (Chen et al., 2021; Sheng et al., 2025). Accordingly, this study treats the river-valley linear form as the background for understanding the overall spatial pattern of the study area and uses the distance to the Yellow River to represent the river-valley location of subdistricts. Previous studies have shown that the association between the built environment and subdistrict-level urban vitality is characterized by both temporal heterogeneity and the joint contribution of multiple factors. The strength of the associations between urban vitality and factors such as transport nodes and commercial functions varies across time periods (Li and Zhao, 2023). Differences in vitality under different temporal contexts are also jointly associated with multidimensional conditions, including functional provision, transport support, and spatial development (Chen et al., 2023; Yang and Wang, 2025), while interaction-enhancement effects may occur among different built environment factors (Ling et al., 2024). The empirical results for Lanzhou further reveal the spatial characteristics of a river-valley linear city: subdistrict-level urban vitality generally extends along the east–west built space, whereas the distance to the Yellow River has relatively low explanatory power for differences in vitality. This indicates that river proximity is insufficient to directly explain differences in vitality among subdistricts, and that the relationship between river-valley topography and urban vitality may be reflected primarily in the overall spatial pattern. Given Lanzhou's urban form, with mountains flanking the city to the north and south and its

built space extending along the river valley, river-valley topography can be regarded as a background condition for the spatial distribution of subdistrict-level urban vitality. Within this spatial context, differences in vitality among subdistricts are mainly associated with transport conditions, functional facilities, and the configuration of built space. Therefore, vitality optimization in river-valley linear cities should consider the characteristics of human activities under different temporal contexts and take an integrated approach to transport connections, functional facilities, and the configuration of built space. This is consistent with the conclusions of previous studies emphasizing the coordinated optimization of multiple built environment elements (Zhang et al., 2025).

This study still has certain limitations. LBS data from a single operator may be affected by differences in user composition, device usage habits, and positioning frequency, making it difficult to fully represent the activity distribution of the entire urban population. The study data cover only May 2025 and therefore cannot reveal seasonal variations or long-term evolution. At the same time, regular weekends and statutory holidays are uniformly classified as rest days, which may weaken differences in activities among types of non-workdays. The existing indicators mainly characterize activity volume and stay intensity and remain insufficient for further identifying activity purposes and behavioral differences among groups differing in age, occupation, and income. The use of subdistrict-level administrative units may also obscure spatial heterogeneity within individual units, and this study has not systematically examined the effects of changes in spatial scale and unit delineation on the analytical results. Furthermore, GeoDetector, random forest, and SHAP mainly reveal spatial associations and predictive contributions and cannot directly determine causal relationships. The use of a single river-valley linear city as a case study also limits the applicability of the research conclusions across other urban forms and stages of development. Future research may further expand multisource and long-term behavioral datasets, differentiate among types of non-workdays and population groups, and examine scale effects using finer spatial units. Future research may also combine multiscale spatiotemporal models with causal identification methods and test the robustness and external applicability of the conclusions through comparative studies of different urban forms.

6.References

[1] Deng Y, Cao K, Chen M, et al. Regulatory effect of China's city hierarchy on urban redevelopment[J]. Nature Cities, 2026: 1-10.

[2] Li J, Burgess G, Sielker F. Political mobilisation and institutional layering in urban regeneration: Transformation of land redevelopment governance in China[J]. Cities, 2023, 141: 104508.

[3] Schläpfer M, Dong L, O'Keeffe K, et al. The universal visitation law of human mobility[J]. Nature, 2021, 593(7860): 522-527.

[4] Sun Honghu, Jiang Yupei. Spatial heterogeneity of the impact of the built environment on urban vitality: A case study of central Nanjing[J]. Geographical Research, 2024, 43(7): 1700-1714.

[5] Jacobs J. The death and life of great American cities[M]. Vintage, 1992.

[6] Cao Zhongming, Zhen Feng, Li Zhixuan, et al. Urban temporal vitality patterns and influencing factors based on mobile phone signaling data: A case study of the central urban area of Nanjing[J]. Human Geography, 2022, 37(6): 109-117. DOI: 10.13959/j.issn.1003-2398.2022.06.013.

[7] Ahas R, Aasa A, Yuan Y, et al. Everyday space–time geographies: using mobile phone-based sensor data to monitor urban activity in Harbin, Paris, and Tallinn[J]. International Journal of Geographical Information Science, 2015, 29(11): 2017-2039.

[8] Wu C, Ye X, Ren F, et al. Check-in behaviour and spatio-temporal vibrancy: An exploratory analysis in Shenzhen, China[J]. Cities, 2018, 77: 104-116.

[9] Li X, Li Y, Jia T, et al. The six dimensions of built environment on urban vitality: Fusion evidence from multi-source data[J]. Cities, 2022, 121: 103482.

[10] Wu C, Ye Y, Gao F, et al. Using street view images to examine the association between human perceptions of locale and urban vitality in Shenzhen, China[J]. Sustainable Cities and Society, 2023, 88: 104291.

[11] Wang Na, Wu Jiansheng, Li Sheng, et al. Spatial characteristics of urban vitality and the influence mechanisms of the built environment based on multisource data: A case study of Shenzhen[J]. Tropical Geography, 2021, 41(6): 1280-1291.

[12] Tang Lu, Xu Hanwei, Ding Yanwen. Comprehensive vitality evaluation of urban blocks integrating multisource geospatial big data[J]. Journal of Geo-information Science, 2022, 24(8): 1575-1588.

[13] Chen Y, Yu B, Shu B, et al. Exploring the spatiotemporal patterns and correlates of urban vitality: Temporal and spatial heterogeneity[J]. Sustainable Cities and Society, 2023, 91: 104440.

[14] Kang C, Fan D, Jiao H. Validating activity, time, and space diversity as essential components of urban vitality[J]. Environment and Planning B: Urban Analytics and City Science, 2021, 48(5): 1180-1197.

[15] Yang J, Wang E. Exploring the nonlinear impacts of built environment on urban vitality from a spatiotemporal perspective at the block scale in Chongqing[J]. ISPRS International Journal of Geo-Information, 2025, 14(6): 225.

[16] Lee S, Cho N. Nonlinear and interaction effects of multi-dimensional street-level built environment features on urban vitality in Seoul[J]. Cities, 2025, 165: 106145.

[17] Chen W, Wu A N, Biljecki F. Classification of urban morphology with deep learning: Application on urban vitality[J]. Computers, Environment and Urban Systems, 2021, 90: 101706.

[18] Yang M, Qian Y, Li X, et al. River valley urban network and morphology: A study on the urban morphology evolution of Lanzhou[J]. Plos one, 2024, 19(5): e0302686.

[19] Lu Bei, Zeng Junwei, Qian Yongsheng, et al. Influence of road network form on urban vitality in the main urban area of Lanzhou City[J]. Arid Land Geography, 2023, 46(8): 1333-1343.

[20] Collins T, Di Clemente R, Gutiérrez-Roig M, et al. Spatiotemporal gender differences in urban vibrancy[J]. Environment and Planning B: Urban Analytics and City Science, 2024, 51(7): 1430-1446.

[21] Yuill R S. The standard deviational ellipse; an updated tool for spatial description[J]. Geografiska Annaler: Series B, Human Geography, 1971, 53(1): 28-39.

[22] Anselin L, Syabri I, Kho Y. GeoDa: an introduction to spatial data analysis[J]. Geographical analysis, 2006, 38(1): 5-22.

[23] Wang J F, Zhang T L, Fu B J. A measure of spatial stratified heterogeneity[J]. Ecological indicators, 2016, 67: 250-256.

[24] Kalange O S, Kahat R S, Kale A S, et al. Implementation of Various Machine Learning Algorithms for Traffic Sign Detection and Recognition[J]. 2022.
[25] Lundberg S M, Erion G, Chen H, et al. From local explanations to global understanding with explainable AI for trees[J]. Nature machine intelligence, 2020, 2(1): 56-67.
[26] Stakhovych S, Bijmolt T H A. Specification of spatial models: A simulation study on weights matrices[J]. Papers in Regional Science, 2009, 88(2): 389-409.
[27] Song Y, Wang J, Ge Y, et al. An optimal parameters-based geographical detector model enhances geographic characteristics of explanatory variables for spatial heterogeneity analysis: Cases with different types of spatial data[J]. GIScience & remote sensing, 2020, 57(5): 593-610.
[28] Sheng J, He Y, Lu T, et al. Unveiling urban vitality and its interactions in mountainous cities: A human behaviour perspective on community-level dynamics[J]. Cities, 2025, 159: 105780.
[29] Li Z, Zhao G. Revealing the spatio-temporal heterogeneity of the association between the built environment and urban vitality in Shenzhen[J]. ISPRS International Journal of Geo-Information, 2023, 12(10): 433.
[30] Zhan D, Wang Y, Wu Q, et al. Nonlinear effects of the urban built environment on urban vitality: A case study of Hangzhou, China[J]. Journal of Geographical Sciences, 2025, 35(6): 1183-1203.
[31] Ling Z, Zheng X, Chen Y, et al. The nonlinear relationship and synergistic effects between built environment and urban vitality at the neighborhood scale: A case study of Guangzhou's central urban area[J]. Remote Sensing, 2024, 16(15): 2826.
[32] Zhang Y, Wang X, Ye Y, et al. Nonlinear relationships and interaction effects of urban built environment on urban vitality based on explainable machine learning[J]. City and Environment Interactions, 2025: 100244.

Data Availability

The LBS trajectory data used in this study were provided by a third-party partner and are managed by the corresponding author's research group. These data are subject to strict non-disclosure agreements (NDAs) and privacy regulations; therefore, they cannot be made publicly available or deposited in any public repository. Subject to the approval of the third-party data provider and compliance with applicable data-use agreements, access may be granted by the corresponding author upon reasonable request and following review and approval by the research group.

Competing interests

The authors declare that they have no conflict of interest.

Ethics statement

This study used anonymized, de-identified LBS data obtained through collaboration with a mobile network operator. All research was conducted in compliance with the Declaration of Helsinki, China's Personal Information Protection Law, and applicable data security and privacy regulations, following a pre-agreed data use protocol. As the data contained no personally identifiable information and the researchers could not identify or contact any data subjects, no human participants were directly recruited. The study was reviewed and approved by the Ethics Review Body of the School of Architecture and Urban Planning, Lanzhou Jiaotong University, which granted a waiver of informed consent.